Structural Characterization and Oxidehydrogenation Activity of CeO2/Al2O3 and V2O5/CeO2/Al2O3 Catalysts

ARTICLE *in* THE JOURNAL OF PHYSICAL CHEMISTRY C · NOVEMBER 2007

Impact Factor: 4.77 · DOI: 10.1021/jp076617l

Structural Characterization and Oxidehydrogenation Activity of CeO_2/Al_2O_3 and $V_2O_5/CeO_2/Al_2O_3$ Catalysts

Benjaram M. Reddy,*,†,‡ Komateedi N. Rao,† Gunugunuri K. Reddy,† Ataullah Khan,†,§ and Sang-Eon Park‡

Inorganic and Physical Chemistry Division, Indian Institute of Chemical Technology, Hyderabad-500007, India, and Laboratory of Nano-Green Catalysis, Department of Chemistry, Inha University, Incheon 402-751, Republic of Korea

Received: August 17, 2007; In Final Form: October 2, 2007

Structural characterization and oxidative dehydrogenation activity of CeO_2/Al_2O_3 and $V_2O_5/CeO_2/Al_2O_3$ catalysts for ethylbenzene (EB) to styrene were investigated systematically. The CeO_2/Al_2O_3 catalyst was prepared by a deposition precipitation method, and a theoretical monolayer equivalent of 10 wt % V_2O_5 was dispersed over its surface by a wet impregnation method to obtain the $V_2O_5/CeO_2/Al_2O_3$ catalyst. To understand thermal and textural stability, the synthesized catalysts were subjected to calcination at various temperatures (773−1073 K). Physicochemical characterization was performed using X-ray diffraction (XRD), Raman spectroscopy (RS), X-ray photoelectron spectroscopy (XPS), thermogravimetric analysis, and BET surface area techniques. The XRD and RS results suggested that the CeO_2/Al_2O_3 sample is thermally quite stable up to 1073 K and that the ceria exists in the form of an over layer on the surface of the alumina support. In the case of the $V_2O_5/CeO_2/Al_2O_3$ sample, no crystalline V_2O_5 was observed from XRD results, indicating a highly dispersed form of vanadium oxide on the CeO_2/Al_2O_3 carrier when calcined at 773 K. The XPS peak shapes and the corresponding electron binding energies indicate that the dispersed vanadium oxide selectively interacts with the ceria portion of the CeO_2/Al_2O_3 support and forms a $CeVO_4$ compound at higher calcination temperatures. Formation of $CeVO_4$ is also established from XRD and RS measurements. Both CeO_2/Al_2O_3 and $V_2O_5/CeO_2/Al_2O_3$ samples were tested for oxidative dehydrogenation of EB to styrene by using dry air as an oxidant. The $V_2O_5/CeO_2/Al_2O_3$ catalyst exhibits more conversion and selectivity than CeO_2/Al_2O_3. The time-on-stream experiments further reveal that the $V_2O_5/CeO_2/Al_2O_3$ catalyst exhibits stable activity and selectivity without fast deactivation.

Introduction

Cerium oxide containing materials have been the subject of numerous investigations in recent years because of their very broad range of applications in catalysis and in advanced ceramic materials.[1−9] Ceria (CeO_2) is a well-known additive as an oxygen storage/release capacity (OSC) material in the so-called three-way-catalysts (TWC) for automobile exhaust treatment.[1,2,8] Also, the CeO_2-based mixed oxides are effective catalysts for oxidation of different hydrocarbons and for the removal of total organic carbon from polluted waters from different sources.[10,11] The presence of CeO_2 promotes various catalytic reactions such as CO_2 activation,[12] CO oxidation,[13,14] CO/NO removal,[15] and low-temperature water−gas shift.[16] The success of ceria in various applications is mainly due to its unique combination of an elevated oxygen transport capacity coupled with the ability to shift easily between reduced and oxidized states ($Ce^{3+} \leftrightarrow Ce^{4+}$).[8] However, the use of pure cerium dioxide is highly discouraged because it is poorly thermostable as it undergoes rapid sintering at high temperatures, thereby losing its crucial OSC characteristics.[8,10,11]

Supported vanadium oxide is a well-known redox catalyst for partial oxidation of various hydrocarbons, ammoxidation of hetro-aromatic compounds, and selective catalytic reduction of NO_x with NH_3.[17−24] Bulk V_2O_5 suffers from poor thermal stability, mechanical strength, and rapid deactivation and promotes nonselective oxidation. Therefore, an appropriate metal oxide support is normally incorporated to vanadium oxide catalysts to overcome those deficiencies.[18,21] In particular, the nature of support has a huge influence on the physicochemical and catalytic properties of the supported vanadium oxide catalysts.[18,21] Although the reaction mechanism of selective oxidation or oxidative dehydrogenation (ODH) has not been established fully, it is widely believed that the breaking of the C−H bond in the hydrocarbon is the rate determining step,[25] and the reaction proceeds via a Mars−Van Krevelen (redox)-type mechanism.[26,27] Further, it is generally agreed that hydrocarbon oxidation over oxide catalysts involves the participation of lattice oxygen species or oxygen vacancies.[21,25,28] Ceria is a well-known oxygen-ion conductor owing to its high concentration of oxygen vacancies and oxygen mobility.[9,27] The CeO_2 containing catalysts have also been reported to display good catalytic properties for oxidative conversion of propane to propylene and ethane to ethylene.[29−31] Therefore, the unique combination of excellent OSC features of CeO_2 and the oxidizing ability of dispersed vanadium oxide is expected to result in a good catalytic system with numerous application

* Corresponding author. E-mail: bmreddy@iict.res.in or mreddyb@yahoo.com.
† Indian Institute of Chemical Technology.
‡ Inha University.
§ Present address: Chemical and Materials Engineering Department, University of Cincinnati, Cincinnati, OH 45221.

10.1021/jp076617l CCC: $37.00
Published on Web 11/28/2007

prospects. The present investigation was undertaken against the aforementioned background. In this study, a CeO_2/Al_2O_3 mixed oxide support was synthesized through a soft-chemical route by adopting a deposition coprecipitation method, and a theoretical monolayer equivalent of V_2O_5 (10 wt %) was deposited over the calcined support (773 K) by a wet impregnation method. The prepared CeO_2/Al_2O_3 and $V_2O_5/CeO_2/Al_2O_3$ samples were subjected to thermal treatments from 773 to 1073 K to understand the dispersion and temperature stability of these materials. The structural evolution was investigated by using X-ray diffraction (XRD), Raman spectroscopy (RS), X-ray photoelectron spectroscopy (XPS), thermogravimetric analysis (TGA), and BET surface area methods. The catalytic performance was evaluated for the ODH of ethylbenzene (EB) to styrene in the vapor phase under normal atmospheric pressure using air as an oxidant.

Styrene is an important monomer extensively used in the chemistry industry for the manufacture of polymers, copolymers, and reinforced plastics.[32,33] Styrene stands fourth place in the series of most used monomers, after ethylene, vinyl chloride, and propylene. Styrene is normally produced by two methods: mainly by dehydrogenation (DH) of EB and as a coproduct of propylene oxide production.[32] The commercial catalyst formulation used for DH of EB is a mixture of iron oxide and potassium carbonate with small quantities of promoters: Cr_2O_3, Ce_2O_3, MoO_3, CaO, MgO, and V_2O_5.[32] The ODH of EB is a third possibility to produce styrene employing different oxidants, which has gained much attention recently.[34−38] The advantage of the ODH process is that, unlike the endothermic DH process, it can be operated at a lower temperature, as it is exothermic.

Experimental Procedures

Catalyst Preparation. CeO_2/Al_2O_3 (1:1 mol ratio based on oxides) was prepared by a deposition precipitation method. In a typical preparation, the requisite quantity of finely powdered γ-Al_2O_3 (Harshaw, surface area (SA) = 208 m^2 g^{-1}) was dispersed in deionized water, to which a calculated amount of ammonium cerium(IV) nitrate (Fluka, AR grade) dissolved in doubly distilled water was added and agitated mechanically for 2 h. To this mixture, a solution of dilute aqueous ammonia was added dropwise under mechanical agitation until precipitation was complete (pH 8.5). The obtained product was filtered off and washed several times with deionized water until it was free from anion impurities. The obtained cake was oven dried at 393 K for 12 h and finally calcined at 773 K for 5 h in air. The $V_2O_5/CeO_2/Al_2O_3$ sample was prepared by a standard wet-impregnation method. To impregnate nominal 10 wt % V_2O_5 over the CeO_2/Al_2O_3 support (773 K calcined), the calculated amount of NH_4VO_3 (Fluka, AR grade) was dissolved in 0.2 M aqueous oxalic acid solution, to which the finely powdered support was added. The excess water was evaporated on a water-bath under vigorous stirring. The resulting material was oven dried at 393 K for 12 h and subsequently calcined at 773 K for 5 h in oxygen atmosphere. Some portions of the support and the finished catalyst were again heated at 873, 973, and 1073 K for 5 h. The rate of heating as well as cooling was always maintained at 5 K min^{-1}.

Catalyst Characterization. The TGA measurements were made on a Mettler Toledo TG-SDTA instrument. The sample (ca. 15 mg) was heated from ambient to 1273 K under N_2 flow, and the heating rate was 10 K min^{-1}. The BET surface area measurements were made by N_2 adsorption at liquid-nitrogen temperature using a Micromeritics Gemini 2360 instrument. Prior to analysis, samples were oven dried at 393 K for 12 h and flushed with argon gas for 2 h. Powder XRD patterns were obtained on Siemens D-5005 and Rigaku MultiFlex instruments using a nickel-filtered Cu Kα (0.15418 nm) radiation source. The intensity data were collected over a 2θ range of 3−80° with a 0.02° step size and using a counting time of 1 s per point. Crystalline phases were identified by comparison with the reference data from the International Center for Diffraction Data (ICDD) files. The average crystallite size of CeO_2 was estimated with the help of the Scherrer equation using the XRD data of all prominent lines.[39] The cell *a* parameter values were calculated by a standard cubic indexation method using the intensity of the ceria base peak (111). The Raman spectra were obtained on a DILOR XY spectrometer equipped with a liquid-nitrogen cooled CCD detector at ambient temperature and pressure. The emission line at 514.5 nm from the Ar^+ ion laser (Spectra Physics) was focused on the sample under a microscope. The power of the incident beam on the sample was 3 mW, and the time of acquisition was adjusted according to the intensity of the Raman scattering. The XPS measurements were performed on a Shimadzu (ESCA 3400) spectrometer by using Mg Kα (1253.6 eV) radiation as the excitation source. The XPS analysis was performed at ambient temperature and pressures typically on the order of less than 10^{-6} Torr. Charging of catalyst samples was corrected by setting the binding energy of the adventitious carbon (C 1s) at 284.6 eV.[40,41]

Catalytic Activity. The catalytic activity for the vapor-phase ODH of EB was carried out in a downflow fixed-bed microreactor under normal atmospheric pressure. In a typical experiment, ca. 0.2 g of the sample mixed with twice the amount of quartz powder was secured between two plugs of Pyrex glass wool inside the glass reactor (Pyrex glass tube, o.d. of 1 cm and i.d. of 0.8 cm) and above the catalyst bed filled with ceramic beads to act as a preheating zone. The reactor was placed vertically inside a tubular furnace, which could be heated electrically and connected to a temperature indicator−controller. The catalyst was pre-activated in a flow of dry air at 773 K for 5 h prior to the reaction. After the activation, the temperature was adjusted to the desired level, and EB was fed from a motorized syringe pump (Perfusor Secura FT) into the vaporizer where it was allowed to mix uniformly with dry air (40−60 mL min^{-1}) before entering the preheating zone of the reactor. The reaction products were analyzed by GC-MS with a flame ionization detector. The conversion and selectivity were calculated as per the procedure described elsewhere.[42]

Results and Discussion

The as-synthesized CeO_2/Al_2O_3 sample before calcination was subjected to TGA analysis. The obtained thermogram between ambient to 1273 K revealed one major and two minor weight loss peaks. The first major weight loss peak in the range of 303−473 K was primarily due to non-dissociative adsorbed water as well as water held on the surface by hydrogen bonding. The second minor weight loss peak between 533−570 K was due to loss of water held in the micropores of the mixed oxide gel. The dehydroxylation of the surface leads to an observed peak in the range of 624−733 K. The TG data revealed ~10% weight loss from ambient to 480 K, ~4% from 480 to 570 K, and ~3.5% from 570 to 773 K, respectively. However, the weight loss from 733 to 1273 K was only ~0.6%, which indicates that over the temperature range between 773 and 1273 K, the sample is thermally quite stable in terms of chemical composition.

The N_2 BET surface areas of various samples prepared in this study and calcined at 773−1073 K are summarized in Table

TABLE 1: BET Surface Area and Crystallite Size Measurements of CeO_2 in CeO_2/Al_2O_3 and $V_2O_5/CeO_2/Al_2O_3$ Samples Calcined at Various Temperatures

sample	BET SA ($m^2\ g^{-1}$)	crystallite size[a] (nm)	cell parameter (Å)
	773 K		
CeO_2/Al_2O_3	158	3.7	5.424
$V_2O_5/CeO_2/Al_2O_3$	69	5.1	n.d.[b]
	873 K		
CeO_2/Al_2O_3	97	4.5	5.417
$V_2O_5/CeO_2/Al_2O_3$	51	17.3	n.d.[b]
	973 K		
CeO_2/Al_2O_3	64	6.3	5.412
$V_2O_5/CeO_2/Al_2O_3$	38	36.5	n.d.[b]
	1073 K		
CeO_2/Al_2O_3	48	11.8	5.398
$V_2O_5/CeO_2/Al_2O_3$	22	51.7	n.d.[b]

[a] From XRD measurements. [b] n.d.: not determined due to compositional heterogeneity.

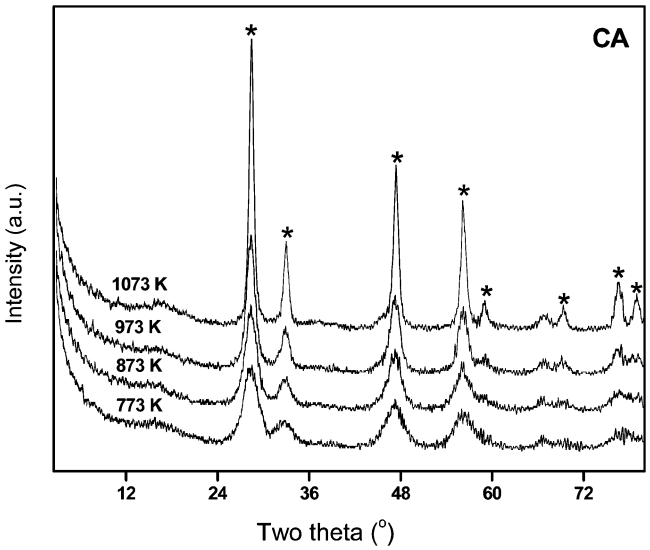

Figure 1. X-ray powder diffraction patterns of CeO_2/Al_2O_3 (CA) sample calcined at different temperatures: (*) lines due to CeO_2.

1. The 773 K calcined CeO_2/Al_2O_3 sample exhibited a high specific surface area of 158 $m^2\ g^{-1}$. As the calcination temperature increased from 773 to 1073 K, a monotonous loss (~69%) in the surface area was observed, which could be attributed to crystallization of ceria and plugging of the alumina pores by the crystallized ceria. Upon impregnation of the CeO_2/Al_2O_3 support with V_2O_5, a substantial loss in the SA could be noted. This is a general phenomenon observed in the case of supported catalysts when an active component is impregnated over its surface.[18] The observed decrease is mainly due to penetration of the dispersed vanadium oxide into the pores of the support, thereby narrowing its pore diameter and blocking some of the micropores.[18,43] The subsequent decline in the surface area upon thermal treatments at higher calcination temperatures could be attributed to particle growth (sintering) and solid-state interactions between the dispersed vanadium oxide and the supporting oxides.[43] The XRD and RS measurements described in the following paragraphs strongly support the latter possibility.

The X-ray powder diffraction pattern of the CeO_2/Al_2O_3 sample calcined at various temperatures is shown in Figure 1. As can be noted from Figure 1, the 773 K calcined sample is in a poorly crystalline form. Only the broad diffraction lines due to CeO_2 (PDF−ICDD 34−-0394) are visible. With increasing calcination temperature from 773 to 1073 K, a gradual increase in the intensity of the lines due to better crystallization of CeO_2 could be noted. Interestingly, no peaks pertaining to the γ-Al_2O_3 phase could be observed from the XRD data. Additionally, no crystalline bulk structures corresponding to interacting species between ceria and alumina could be observed. According to the literature, temperatures below 600 K are not thermodynamically favorable for the reduction of ceria into CeO_x and the formation of $CeAlO_3$.[44] However, within the temperature range of 673−973 K, the non-stoichiometric CeO_{2-x} formation is most favorable. Temperatures above 800 K favor the formation of $CeAlO_3$. As suggested by Humbert et al.,[44] the nucleation of $CeAlO_3$ occurs by diffusion of Al^{3+} ions into the partially reduced CeO_2 lattice. The small size of Al^{3+} as compared to Ce^{3+} makes the diffusion easy. On the other hand, incorporation of Ce^{3+} ions in the vacant positions of the alumina lattice is also possible. According to the model proposed by Humbert et al.,[44] the geometrical arrangement between the three structures of CeO_2, $CeAlO_3$, and transition Al_2O_3 also favor the formation of cerium aluminate at the interface. However, in the present study, there is no evidence for the formation of the $CeAlO_3$ phase, which could be due to a different preparation method adopted and the calcination conditions employed.

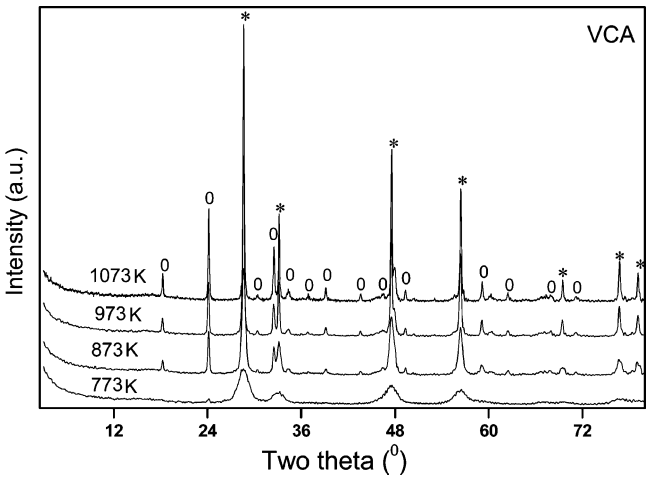

Figure 2. X-ray powder diffraction patterns of $V_2O_5/CeO_2/Al_2O_3$ sample calcined at different temperatures: (*) lines due to CeO_2 and (0) lines due to $CeVO_4$.

Figure 2 represents the X-ray diffraction patterns of the $V_2O_5/CeO_2/Al_2O_3$ sample calcined at different temperatures. The 773 K sample reveals only broad diffraction lines due to CeO_2. No lines due to the crystalline V_2O_5 phase indicate the presence of a highly dispersed and amorphous vanadium oxide species on the surface of the support. However, with increasing calcination temperature, the intensity of the CeO_2 diffraction lines increased sharply. Also, a few new diffraction peaks due to the formation of $CeVO_4$ could be observed. The intensity of these lines increased with increasing calcination temperature on account of better crystallization.[45] Selective formation of $CeVO_4$ demonstrates the affinity of dispersed vanadium oxide toward ceria instead of alumina, leading to the facile formation of $CeVO_4$ as against $AlVO_4$.

The crystallite size (D_{XRD}) of CeO_2 in the CeO_2/Al_2O_3 and $V_2O_5/CeO_2/Al_2O_3$ samples as a function of calcination temperature is summarized in Table 1. As can be noted from Table 1, the crystallite size of CeO_2 in both the samples increased with increasing calcination temperature. The extent of crystallite growth is greater in the case of the $V_2O_5/CeO_2/Al_2O_3$ sample.This indicates that the impregnated vanadium oxide accelerates the grain growth of ceria in the $V_2O_5/CeO_2/Al_2O_3$

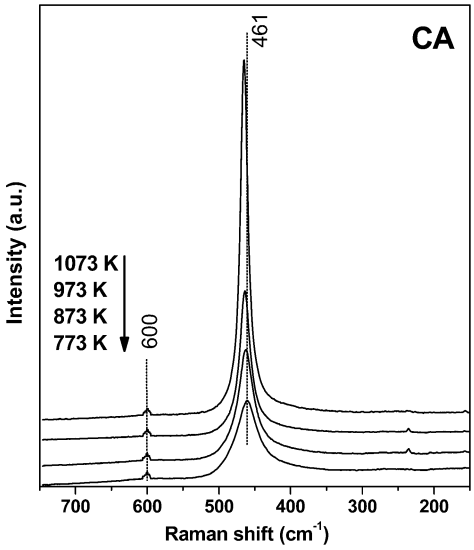

Figure 3. Raman spectra of CeO_2/Al_2O_3 sample calcined at different temperatures.

samples.[18,45] Using the most intense (111) line of the CeO_2 pattern, cubic indexation and calculation of unit cell parameters have been carried out for the CeO_2/Al_2O_3 sample and presented in Table 1.[46,47] These estimations reveal a steady decrease of the cell *a* parameter with increasing calcination temperature, signifying the lattice contraction in agreement with Vegard's law. According to Vegard's rule, a linear decrease of lattice parameter or cell volume is expected due to the insertion of an increasing amount of Al^{3+} into the CeO_2 lattice since the ionic radius of Al^{3+} (0.051 nm) is smaller than that of Ce^{4+} (0.097 nm). However, the XRD technique did not detect any crystalline Ce−Al-oxide compound formation.

The cation order−disorder and lattice distortion can in principle be easily detected by conventional XRD analysis. However, XRD does not allow accurate detection of distortions of oxygen sublattice and/or defects in the structure due to poor sensitivity of the technique to the oxygen atoms in the presence of heavy Ce and Al atoms. Since the mobility of oxygen atoms in the lattice is a critical property for most of the applications of these materials, both as ionic/electronic conductors and redox catalysts, a deeper insight into the fine structural details is desirable. Raman spectroscopy is a powerful technique in this regard. Accordingly, the Raman spectra of various samples prepared in this study have been recorded. As presented in Figure 3, the Raman spectrum of the CeO_2/Al_2O_3 sample calcined at 773 K shows a prominent peak at about 461 cm^{-1} and a weak band at 600 cm^{-1}. The band at 461 cm^{-1} corresponds to triply degenerate F_{2g} mode and can be viewed as a symmetric breathing mode of oxygen atoms around cerium ions.[48] With an increase in calcination temperature from 773 to 1073 K, the band at 461 cm^{-1} shifted to 465 cm^{-1} and became sharp and more symmetrical. This is due to a better crystallization of ceria at higher calcination temperatures, in agreement with XRD measurements. It is a known fact in the literature that the intensity of the Raman band depends on several factors, including the grain size and morphology.[49] The weak band observed at ~600 cm^{-1} corresponds to a doubly degenerate longitudinal optical mode of CeO_2.[50] This band frequently has been linked to oxygen vacancies in the CeO_2 lattice.[35,51] For each sample, the spectra were recorded at several points, and no shift in the band position or difference of width was noted. This observation reveals clearly that the CeO_2/Al_2O_3 sample is homogeneous. In line with XRD measurements, no Raman bands pertaining to alumina or compounds of ceria−alumina were observed. The Raman measurements suggest the existence of a surface over a layer of ceria on the alumina support.

Raman spectra of the $V_2O_5/CeO_2/Al_2O_3$ sample calcined at different temperatures are presented in Figure 4. The 773 K calcined sample exhibits a prominent peak at 464 cm^{-1} and some broad and less intense bands at around 1015−1035, 600, and 230 cm^{-1}, respectively. With an increasing calcination temperature from 773 to 1073 K, sharpening of the band at 464 cm^{-1} and diminishing of a few other bands can be noted. Further, at higher calcination temperatures, some new bands are observed at around 262, 377, 786, 797, and 861 cm^{-1}, which are due to the formation of $CeVO_4$. The intensity of these bands increased with increasing calcination temperature from 973 to 1073 K, owing to an increase in the crystallite size. The band observed at 464 cm^{-1} is due to the F_{2g} mode of the ceria cubic lattice as discussed previously. No crystalline V_2O_5 features (Raman bands at 995, 702, 527, 404, 284, and 146 cm^{-1}) were observed in agreement with the XRD results.[51] As reported in the literature,[52] the band at 1015−1035 cm^{-1} primarily corresponds to an isolated VO_4^{3-} surface species with one terminal V−O bond, the intensity of which is found to decrease with an increasing calcination temperature. It is proposed that the VO_4^{3-} surface species present on the CeO_2/Al_2O_3 carrier will be integrated together under the influence of high-temperature calcination and interact with the ceria to form the stable $CeVO_4$ compound, thereby decreasing the amount of dispersed vanadium oxide on the surface of the support. According to literature reports, tetrahedral VO_4^{3-}, as present in aqueous solution, has the most prominent Raman band at 827 cm^{-1}, and for solids, with isolated VO_4^{3-} units, this band lies in the range of 830−860 cm^{-1}.[53] It is associated with the breathing mode of the vanadium tetrahedron. In $CeVO_4$, vanadium ions are placed at the centers of oxygen tetrahedrally with a vanadium oxygen distance (d_{V-O}) of 1.7 Å similar to that of isolated VO_4^{3-}. Therefore, the band at 860 cm^{-1} of $CeVO_4$ could be assigned to such a mode. The Raman results thus corroborate with the observations made from XRD measurements. They show the formation of $CeVO_4$ in parallel with the disappearance of dispersed vanadium oxide and also the crystallization of CeO_2 at higher calcination temperatures.

To verify the elemental oxidation states, the prepared samples were analyzed by XPS. The electron binding energies (eV) of the photoelectron peaks pertaining to O 1s, Al 2p, Ce 3d, and V 2p are presented in Table 2. The representative photoelectron peaks of O 1s, Ce 3d, and Al 2p are shown in Figures 5−7, respectively. The photoelectron peak shapes and corresponding binding energies are sensitive to the calcination temperature as well as vanadium oxide coverage and agree well with literature reports.[54,55] Figure 5 displays the O 1s spectra of CeO_2/Al_2O_3 and $V_2O_5/CeO_2/Al_2O_3$ samples calcined at different temperatures. The O 1s peak is generally broad and complicated due to the overlapping contribution of oxygen from ceria and alumina in the case of CeO_2/Al_2O_3 and ceria, alumina, and vanadia in the case of $V_2O_5/CeO_2/Al_2O_3$, respectively. The binding energy of the most intense peak, in the case of CeO_2/Al_2O_3, is almost constant with increasing calcination temperature. The observed intense peak at about 530.8 eV mainly belongs to the oxygen atoms that are bound to Ce, judging from the differences in the electronegativity of the elements involved and from the literature.[40,55] The O 1s profile of the $V_2O_5/CeO_2/Al_2O_3$ sample shows much broader and asymmetric peaks at 773−873 K calcination temperatures. The binding energy maxima (530.1−530.2 eV) are fairly constant with increasing calcination temperature. At

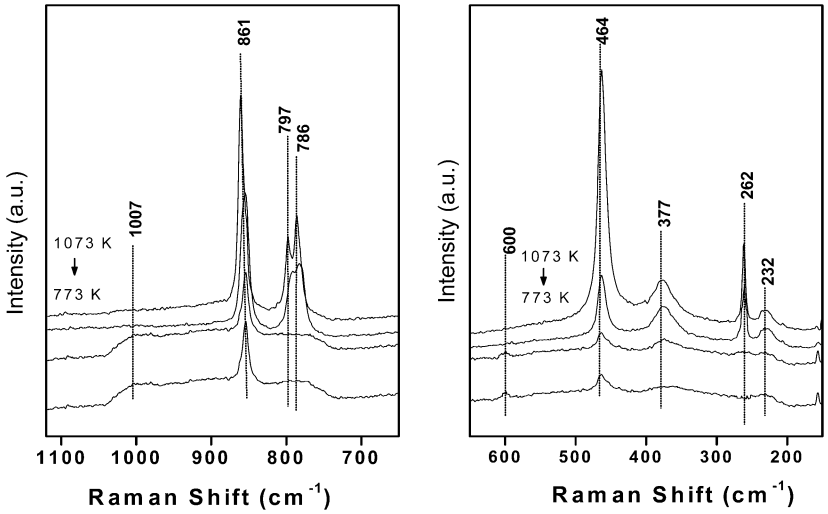

Figure 4. Raman spectra of $V_2O_5/CeO_2/Al_2O_3$ sample calcined at different temperatures and recorded in two separate regions.

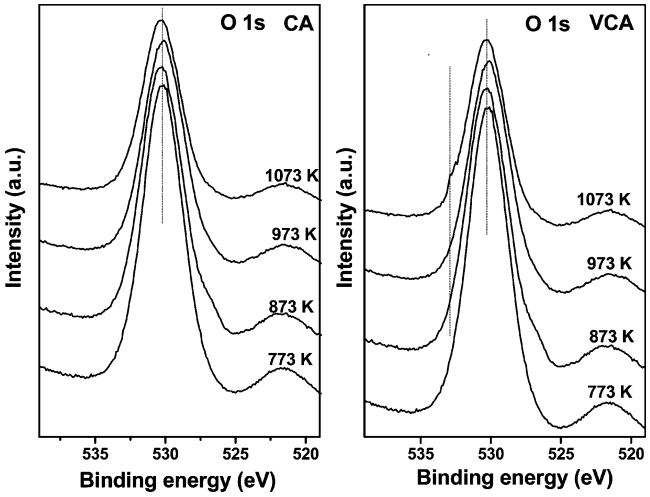

Figure 5. O 1s XPS spectra of CeO_2/Al_2O_3 and $V_2O_5/CeO_2/Al_2O_3$ samples calcined at different temperatures.

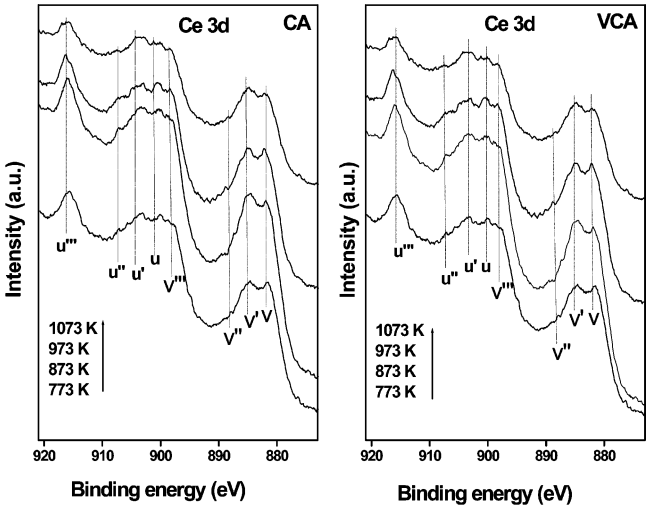

Figure 6. Ce 3d XPS spectra of CeO_2/Al_2O_3 and $V_2O_5/CeO_2/Al_2O_3$ samples calcined at different temperatures.

TABLE 2: XPS Core Level Binding Energies (eV) of CeO_2/Al_2O_3 and $V_2O_5/CeO_2/Al_2O_3$ Samples Calcined at Various Temperatures

	binding energy (eV)			
temp (K)	O 1s	Al 2p	Ce 3d	V 2p
		CeO_2/Al_2O_3		
773	530.8	73.6	881.7	
873	530.7	73.7	881.9	
973	530.6	73.6	882.2	
1073	530.6	73.6	882.1	
		$V_2O_5/CeO_2/Al_2O_3$		
773	530.1	73.3	881.5	517.5
873	530.2	73.6	881.9	517.5
973	530.1	73.3	882.2	517.3
1073	530.2	73.5	882.2	516.8

higher calcination temperatures, the observed broad peak at 532.9 eV could be attributed to the formation of $CeVO_4$, as noted from XRD and Raman measurements.[45]

Typically, the Ce 3d XPS core level spectra exhibit three-lobed envelopes (around 879−890, 895−910, and 916 eV) such as those depicted in Figure 6 for CeO_2/Al_2O_3 and $V_2O_5/CeO_2/Al_2O_3$ catalysts, respectively. From these envelopes, the coexistence of both Ce^{3+} and Ce^{4+} oxidation states is distinguishable, although the 4+ oxidation state is predominant at lower calcination temperatures.[56] Because of the complex shape of the spectrum for nonstoichiometric cerium oxide, it is postulated

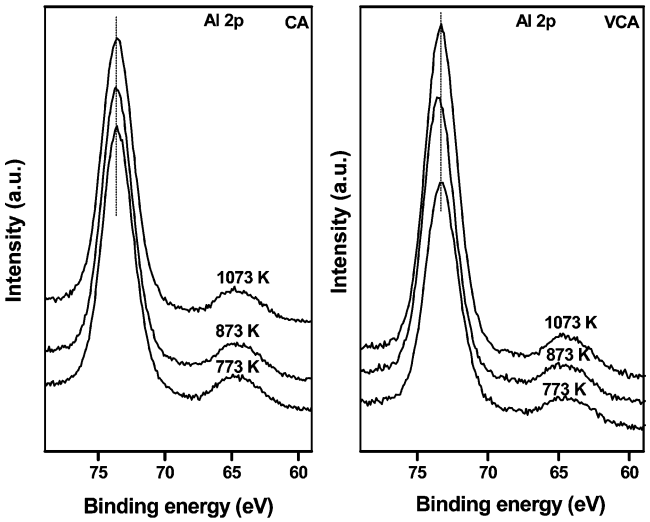

Figure 7. Al 2p XPS spectra of CeO_2/Al_2O_3 and $V_2O_5/CeO_2/Al_2O_3$ samples calcined at different temperatures.

that the Ce 3d spectrum arises from the partially oxidized surface Ce species in the catalysts and can be approximated as a linear combination of the spectra characterizing the stoichiometric oxides with 3+ and 4+ valence states.[57] Further, it can be individually resolved into five sets of features grouped as *u* and

v lines, respectively, to denote the electronic transitions in the $3d_{3/2}$ and $3d_{5/2}$ levels, following the notation of Burroughs et al.[57] The peaks labeled v and v'' have been assigned to a mixing of Ce $3d^9$ $4f^2$ O $2p^4$ and Ce $3d^9$ $4f^1$ O $2p^5$ Ce(IV) final states, and the peak denoted as v''' corresponds to the Ce $3d^9$ $4f^0$ O $2p^6$ Ce(IV) final state. On the other hand, lines v_0 and v' are assigned to the Ce $3d^9$ $4f^2$ O $2p^5$ and Ce $3d^9$ $4f^0$ O $2p^6$ Ce(III) final states. The same assignment can be applied to the u structures, which correspond to the Ce $3d_{3/2}$ levels. As previously pointed out, the XPS spectrum of pure support calcined at 773 K exhibits peaks due to the presence of both Ce^{4+} and Ce^{3+}, thus implying that cerium is present at the surface in both 4+ and 3+ oxidation states. As the calcination temperature increases, the intensity of the u''' peak decreases, and the intensity of the u' and v' annotated peaks increases, indicating an increase in the surface content of Ce^{3+}. Most likely, Ce(III) has been formed due to the reduction of Ce(IV) under the conditions of ultrahigh vacuum during XPS measurements in conformity with earlier reports in the literature.[58,59] However, the presence of Ce_2O_3 (Ce^{3+}) was not observed from the XRD measurements. The Ce 3d spectra of $V_2O_5/CeO_2/Al_2O_3$ also show two broad overlapping regions; one located between 877 and 890 eV and a second between 895 and 909 eV, primarily indicating the existence of Ce^{3+}/Ce^{4+} oxidation states. With increasing calcination temperature, the relative intensity of the peaks pertaining to Ce^{3+} increased marginally at the expense of the Ce^{4+} peaks.[60]

As presented in the Table 2, the binding energy of the Al 2p photoelectron peak ranged between 73.3 and 73.6 eV for the CeO_2/Al_2O_3 and $V_2O_5/CeO_2/Al_2O_3$ samples, respectively, which agrees well with literature reports.[40,61] As shown in Figure 7, the spectra are relatively broad, indicating that alumina is not easily accessible at the surface due to the presence of the ceria over layer. With increasing calcination temperature, a slight increase in the intensity of the Al 2p peak is observed. This is mainly due to better crystallization and redistribution of various components in the samples under the influence of high-temperature calcination. Further, no large change in the Al 2p binding energies indicates that there is no evidence for compound formation between alumina and other component oxides. The XPS spectrum of V 2p pertaining to $V_2O_5/CeO_2/Al_2O_3$ samples was very broad due to the presence of multiple oxidation states and electron transfer between the active component and the support.[18,62] However, the intensity of the V 2p band was found to increase with increasing calcination temperature. With increasing calcination temperature from 773 to 1073 K, the binding energy of V 2p decreased from 517.5 to 516.8 eV. According to the literature, the binding energy of V 2p reported for V_2O_5 (V^{5+} oxidation state) ranges between 517.4 and 516.4 eV; the next oxidation state, V^{4+}, represented by V_2O_4, shows values in the range of 515.7−515.4 eV.[62] As presented in Table 2, there is a slight shift from 517.5 to 516.8 eV with increasing calcination temperature, which indicates a progressive reduction of the V species at the surface under the influence of high-temperature calcination.

The preferential formation of $CeVO_4$ at higher calcination temperatures, due to solid-state reaction between the dispersed vanadium oxide and the ceria portion of the CeO_2/Al_2O_3 mixed oxide, seems to be an interesting observation in this study. $CeVO_4$ has been reported to exhibit interesting catalytic behavior for certain selective oxidation reactions.[29] The formation of the $CeVO_4$ phase can be explained by taking into account the charge-to-radius ratio of the mixed oxides as envisaged by Bond and Tahir.[18] The formation of surface compounds or uni-

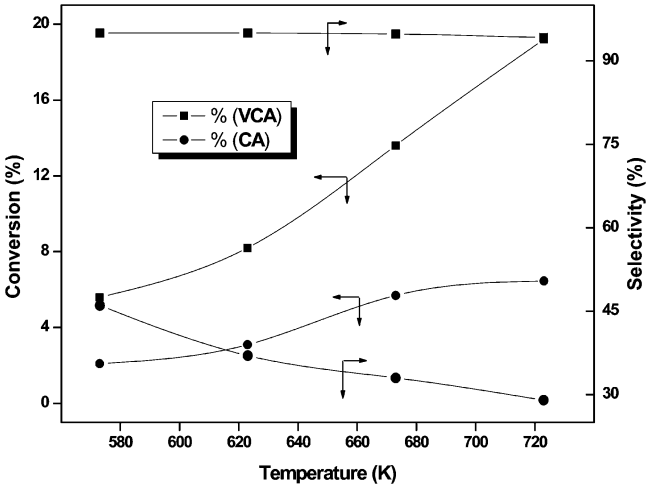

Figure 8. Oxidative dehydrogenation activity of (a) CeO_2/Al_2O_3 and (b) $V_2O_5/CeO_2/Al_2O_3$ catalysts as a function of reaction temperature.

dimensional layers of vanadium oxide on various oxide supports has been related to the ratio of the charge of the support cation to the sum of the radii of the cation and oxide ions (q/r).[18] Normally, lower q/r ratios favor surface compound formation. The q/r ratio for the vanadia−ceria combination is lower because the radius of Ce^{4+} is higher than that of Al^{3+}. Therefore, the dispersed vanadium oxide is expected to interact selectively with the ceria portion of the mixed oxide, thereby leading to the formation of the $CeVO_4$ surface compound.

Supported vanadium oxide catalysts are known to catalyze the ODH of alkanes with high activity and selectivity. Interestingly, the oxidant used in the ODH reaction also plays a crucial role in determining the activity, selectivity, and stability of the catalysts. The use of O_2, CO_2, SO_2, N_2, dry air, and N_2O gases as oxidants has been investigated for the ODH processes.[34,35,37,38,63] The application of O_2 and SO_2 leads to deep oxidation of ethylbenzene to CO_x and the formation of toxic side products, respectively.[63] CO_2 as an oxidant is believed to result in the formation of carbonaceous deposits resulting in fast deactivation of the catalyst, and N_2O leads to more styrene oxide selectivity.[34] On the other hand, the use of pure N_2 suffers from the availability of oxygen, resulting in low product yields. Dry air is generally preferred as an oxidant due to its low cost and easy handling. In the present investigation, the ODH of EB was carried out using dry air as an oxidant as this study was primarily aimed at understanding the role of ceria on vanadium oxide when impregnated over an alumina support.

The plausible products that can be expected during the ODH of EB are styrene (desired product), benzaldehyde, benzoic acid, acetophenone, toluene, benzene, carbon monoxide, and carbon dioxide (undesired side products).[37,38] Preliminary tests revealed that the ODH of EB was negligible in the absence of any catalyst, in a wide range of temperatures. Interestingly, in the present study under the experimental conditions employed, styrene formed a major part of the reaction product. Only a small quantity of other products and CO_2 was noted. The catalytic activity of CeO_2/Al_2O_3 and $V_2O_5/CeO_2/Al_2O_3$ samples calcined at 773 K was measured over the temperature range of 573−723 K, and the conversion of EB and the selectivity toward styrene were recorded at different temperatures. Figure 8 shows the EB conversion and styrene selectivity as a function of temperature. In general, an increase in the conversion with an increase of temperature was observed. The conversion of EB and selectivity to styrene over CeO_2/Al_2O_3 was relatively lower when compared to the vanadia impregnated sample. Also, the

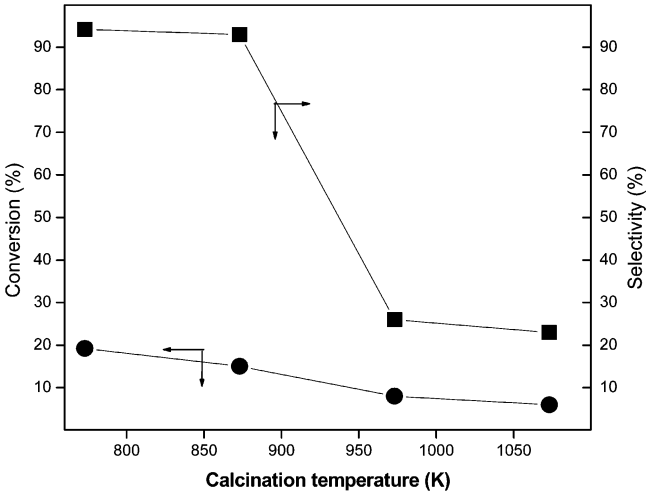

Figure 9. Oxidative dehydrogenation activity of $V_2O_5/CeO_2/Al_2O_3$ catalyst calcined at different temperatures.

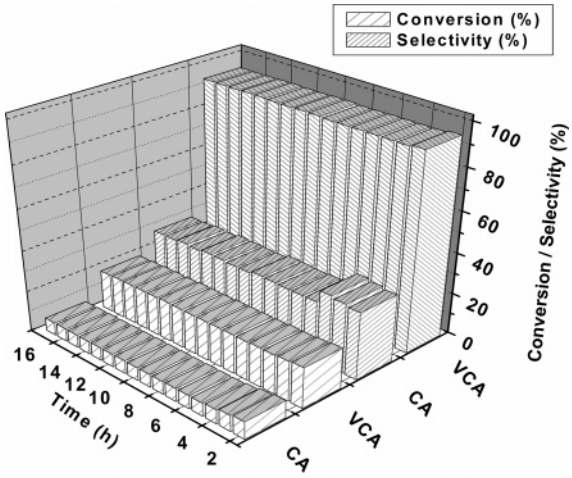

Figure 10. Oxidative dehydrogenation activity of (a) CeO_2/Al_2O_3 and (b) $V_2O_5/CeO_2/Al_2O_3$ catalysts as a function of time-on-stream.

selectivity of styrene decreased with increasing temperature over CeO_2/Al_2O_3 and remained almost constant over the vanadia containing sample. The influence of space velocity (changing EB feed rate) on the conversion and selectivity of the catalysts was also investigated at 723 K in the range of 0.5−2.0 h^{-1}. As expected, the conversion decreased with increasing space velocity. The decrease in the conversion was primarily due to a shorter contact time of the reactants on the catalyst surface with increasing space velocity. The selectivity to styrene increased from 0.5 to 1 h^{-1} space velocity and remained constant up to 2 h^{-1}. The reaction was also carried out by using the $V_2O_5/CeO_2/Al_2O_3$ catalyst calcined at different temperatures to understand the effect of calcination temperature. The activity and selectivity profiles are illustrated in Figure 9. The conversion as well as selectivity decreased at high calcination temperatures. The selectivity was almost constant for 773 and 873 K calcined samples and decreased rapidly for 973 and 1073 K samples. The formation of toluene, benzaldehyde, benzoic acid, and other side products were observed for 973 and 1073 K calcined samples. This may be due to sintering of the samples at higher calcintion temperatures, leading to loss of specific surface area and also due to the formation of the cerium vanadate compound. The formation of $CeVO_4$ at higher calcination temperatures was supported by XRD, Raman, and XPS techniques.

The time-on-stream experiments revealed a stable catalytic behavior of the $V_2O_5/CeO_2/Al_2O_3$ sample toward the ODH of EB, as shown in Figure 10. As can be noted from Figure 10, the conversion and selectivity of styrene in the time-on-stream experiments remained almost constant within the investigated time limits (16 h), indicating a quite stable activity. The sum of the selectivities of dealkylation side products was also found to remain less and does not show any appreciable increase with time-on-stream. These results reveal a good catalytic efficiency of V_2O_5 without deactivation when supported on the CeO_2/Al_2O_3 carrier. A fast deactivation is noted in most of the cases during time-on-stream experiments on various catalyst systems.[41] It has been observed in a few cases in the literature that the ODH activity improves with time (TOS studies) on account of the formation of a thin layer of carbonaceous deposit, which promotes the ODH activity or reaction.[64] However, no such surface carbonaceous deposit formation was noted in the present study, which is authenticated by the fact that the activity remained constant over extended periods of time (Figure 10). In fact, there was no weight gain in the catalyst at the end of the reaction for several hours, and the color of the catalyst also did not change. The vanadia-free CeO_2/Al_2O_3 catalyst exhibited poor selectivity toward styrene and promoted the formation of CO_2. Recent literature reports also reveal that the ceria−zirconia mixed oxide support can produce a stable catalytic activity during time-on-stream runs. The NiO_x/Ce−Zr oxide catalyst exhibited a stable activity for syn-gas production via CO_2 reforming of methane without a significant loss during time-on-stream runs.[65] Similar trends were noticed for the partial oxidation of methane,[66] dehydration of 4-methyl-2-pentanol,[67] and methane combustion.[29] On the contrary, a rapid deactivation was noticed in the case of the VO_x/Al_2O_3 catalyst.[34] The stable activity in the cerium oxide containing catalysts could be attributed to the facile oxygen transport from the bulk of cerium oxide solid solutions that help in the prevention of coke formation, which is the main deactivation pathway of these catalysts. Thus, the obtained stable activity for the ODH of EB in the present study is in good agreement with the literature reports. The remarkable ability of CeO_2/Al_2O_3 to stabilize the catalytic activity of dispersed vanadium oxide is clearly apparent from the present study.

Conclusion

The CeO_2/Al_2O_3 sample obtained by a deposition precipitation method exhibits reasonably high specific surface area and high thermal stability up to 1073 K calcination temperature. The characterization results suggest that ceria forms an over layer on the surface of the alumina support. The CeO_2/Al_2O_3 composite oxide is also a good carrier for the dispersion of vanadium oxide. The impregnated vanadium oxide (10 wt %) is observed to be in a highly dispersed state on the surface of the support when calcined at 773 K. No crystalline V_2O_5 could be noted from XRD and Raman measurements. The dispersed vanadium oxide interacts selectively with the ceria portion of the CeO_2/Al_2O_3 carrier and readily forms a stable $CeVO_4$ compound. The XPS measurements revealed that both aluminum and vanadium are in their highest oxidation states, Al^{3+} and V^{5+}, respectively. However, cerium displays the presence of both Ce^{4+} and Ce^{3+} oxidation states in different proportions depending on the presence/absence of vanadium oxide and the calcination temperature employed. The $V_2O_5/CeO_2/Al_2O_3$ catalyst exhibits good activity and selectivity for the oxidative dehydrogenation of ethylbenzene to styrene. Further, the $V_2O_5/CeO_2/Al_2O_3$ combination catalyst is more active than CeO_2/Al_2O_3 and found to exhibit quite stable activity in the time-on-stream experiments. Further studies are essential to understand

the significance of ceria in oxidation catalysts to prevent catalyst deactivation and to enhance the activity and selectivity of the catalysts.

Acknowledgment. We thank Dr. S. Loridant, IRCE-Lyon, France, and Dr. Y. Yamada, AIST-Osaka, Japan, for providing Raman and XPS results, respectively. B.M.R. thanks the Korea Federation of Science and Technology, South Korea, for a visiting fellowship under the Brain Pool program. G.K.R. and K.N.R. thank UGC, New Delhi, for Research Fellowships.

References and Notes

(1) Trovarelli, A. *Catalysis by Ceria and Related Materials*; Catalytic Science Series 2; World Scientific Publishing Company: London, 2002.
(2) Bernal, S.; Kasper, J.; Trovarelli, A. *Catal. Today* **1999**, *50*, 173.
(3) Trovarelli, A. *Catal. Rev. Sci. Eng.* **1996**, *38*, 439 and references therein.
(4) Sato, T.; Dosaka, K.; Ishitsuka, M.; Haga, E. M.; Okuwaki, A. *J. Alloys Compd.* **1993**, *193*, 274.
(5) Sahibzada, M.; Steele, B. C. H.; Zheng, K.; Rudkin, R. A.; Metcalfe, I. S. *Catal. Today* **1997**, *38*, 459.
(6) Rossignol, S.; Madier, Y.; Duprez, D. *Catal. Today* **1999**, *50*, 261.
(7) Fornasiero, P.; Balducci, G.; Di Monte, R.; Kaspar, J.; Sergo, V.; Gubitosa, G.; Ferrero, A.; Graziani, M. *J. Catal.* **1995**, *164*, 173.
(8) Trovarelli, A.; de Leitenburg, C.; Dolcetti, G. *CHEMTECH* **1997**, *27*, 32.
(9) Taylor, K. C. *Catalysis Science and Technology*; Springer-Verlag: Berlin 1984; Ch. 2.
(10) Imamura, S.; Fakuda, I.; Ishida, S. *Ind. Eng. Chem. Res.* **1988**, *27*, 718.
(11) Mishra, V. S.; Mahajani, V. V.; Joshi, J. B. *Ind. Eng. Chem. Res.* **1995**, *34*, 2.
(12) Trovarelli, A.; Dolcetti, G.; de Leitenburg, C.; Kaspar, J.; Finetti, P.; Santoni, A. *J. Chem. Soc., Faraday Trans. 1* **1992**, *88*, 1311.
(13) Reddy, B. M.; Bharali, P.; Saikia, P.; Khan, A.; Loridant, S.; Muhler, M.; Grünert, W. *J. Phys. Chem. C* **2007**, *111*, 10478.
(14) Monteiro, R. S.; Dieguez, L. C.; Schmal, M. *Catal. Today* **2001**, *65*, 77.
(15) Zhang, H.; Zhu, A.; Wang, X.; Wang, Y.; Shi, C. *Catal. Commun.* **2007**, *8*, 612.
(16) Andreeva, D.; Ivanov, I.; Abrashov, M. V. *Appl. Catal., A* **2006**, *302*, 127.
(17) Guliants, V. V. *Catal. Today* **1999**, *51*, 255.
(18) Bond, G. C.; Tahir, S. F. *Appl. Catal.* **1991**, *71*, 1 and references therein.
(19) Deo, G.; Wachs, I. E.; Haber, J. *Crit. Rev. Surf. Chem.* **1994**, *4*, 141.
(20) Hucknall, D. J. *Selective Oxidation of Hydrocarbons*; Academic Press: London, 1974.
(21) Reddy, B. M. Redox Properties of Metal Oxides. In *Metal Oxides: Chemistry and Applications*; Fierro, J. L. G., Ed.; CRC Press: Boca Raton, FL, 2006; Ch. 8, p 215.
(22) Reddy, B. M.; Lakshmanan, P.; Khan, A. *J. Phys. Chem. B* **2004**, *108*, 16855.
(23) Reddy, B. N.; Reddy, B. M.; Subrahmanyam, M. *J. Chem. Soc., Faraday Trans.* **1991**, *87*, 1649.
(24) Corma, A.; Lopez Nieto, J. M.; Paredes, N. *J. Catal.* **1993**, *144*, 425.
(25) Chen, K.; Iglesia, E.; Bell, A. T. *J. Catal.* **2000**, *192*, 197.
(26) Chen, K.; Khodakov, A.; Yang, J.; Bell, A. T.; Iglesia, E. *J. Catal.* **1999**, *186*, 325.
(27) Kung, H. H. *Adv. Catal.* **1994**, *40*, 1.
(28) Bielanski, A.; Haber, J. *Oxygen in Catalysis*, 2nd ed.; Marcel Dekker: New York, 1990.
(29) Daniell, W.; Ponchel, A.; Kuba, S.; Anderle, F.; Weingand, T.; Gregory, D. H.; Knözinger, H. *Top. Catal.* **2002**, *20*, 65.
(30) Feng, T.; Vohs, J. M. *J. Catal.* **2004**, *221*, 619.
(31) Burcham, L. J.; Deo, G.; Gao, X.; Wachs, I. E. *Top. Catal.* **2000**, *11*−*12*, 85.
(32) Lee, E. H. *Catal. Rev.* **1973**, *8*, 285.
(33) Cavani, F.; Trifiro, F. *Appl. Catal., A* **1995**, *133*, 219.
(34) Shiju, N. R.; Anilkumar, M.; Mirajkar, S. P.; Gopinath, C. S.; Rao, B. S.; Satyanarayana, C. V. *J. Catal.* **2005**, *230*, 484 and references therein.
(35) Reddy, B. M.; Lakshmanan, P.; Loridant, S.; Yamada, Y.; Kobayashi, T.; Cartes, C. L.; Rojas, T. C.; Fernandez, A. *J. Phys. Chem. B* **2006**, *110*, 9140.
(36) Chang, W. S.; Chen, Y. Z.; Yang, B. L. *Appl. Catal., A* **1995**, *124*, 221.
(37) Burry, D. R.; Cho, K.-M.; Han, S.-C.; Koo, J.-B.; Park, S.-E. *Catal. Today* **2006**, *115*, 242.
(38) Park, S.-E.; Han, S.-C. *J. Ind. Eng. Chem.* **2004**, *10*, 1257.
(39) Klug, H. P.; Alexander, L. E. *X-ray Diffraction Procedures for Polycrystalline and Amorphous Materials*, 2nd ed.; John Wiley and Sons: New York, 1974.
(40) Briggs, D.; Seah, M. P. Practical Surface Analysis, In *Auger and X-Ray Photoelectron Spectroscopy*, 2nd ed.; Wiley, New York, 1990; Vol. 1.
(41) Wagner, C. D.; Riggs, W. M.; Davis, L. E.; Moulder, J. F. In *Handbook of X-Ray Photoelectron Spectroscopy*; Muilenberg, G. E., Ed.; PerkinElmer Corporation: Waltham, MA, 1978.
(42) Reddy, B. M.; Ganesh, I. *J. Mol. Catal. A: Chem.* **2001**, *169*, 207.
(43) Reddy, B. M.; Ganesh, I.; Reddy, E. P. *J. Phys. Chem. B* **1997**, *101*, 1769.
(44) Humbert, S.; Colin, A.; Monceaux, L.; Ovdet, F.; Courtine, P. *Stud. Surf. Sci. Catal.* **1995**, *96*, 829.
(45) Reddy, B. M.; Khan, A.; Yamada, Y.; Kobayashi, T.; Loridant, S.; Volta, J.-C. *J. Phys. Chem. B* **2002**, *106*, 10964.
(46) Bozo, C.; Gaillard, F.; Guilhaume, N. *Appl. Catal., A* **2001**, *220*, 69.
(47) Colon, G.; Pijolat, M.; Valdivieso, F.; Vidal, H.; Kaspar, J.; Finocchio, E.; Daturi, M.; Binet, C.; Lavalley, J. C.; Baker, R. T.; Bernal, S. *J. Chem. Soc., Faraday Trans.* **1998**, *94*, 3717.
(48) Lin, X.-M.; Li, L.-P.; Li, G.-S.; Su, W.-H. *Mater. Chem. Phys.* **2001**, *69*, 236.
(49) Spanier, J. E.; Robinson, R. D.; Zhang, F.; Chan, S.-W.; Herman, I. P. *Phys. Rev. B* **2001**, *64*, 54071.
(50) McBride, J. R.; Hass, K. C.; Poindexter, B. D.; Weber, W. H. *J. Appl. Phys.* **1994**, *76*, 2435.
(51) Jehng. J.-M. *J. Phys. Chem. B* **1998**, *102*, 5816.
(52) Eckert, H.; Wachs, I. E. *J. Phys. Chem.* **1989**, *93*, 6796.
(53) Griffith, W. P.; Lesniak, P. J. B. *J. Chem. Soc. A* **1969**, 1066.
(54) Fereres, M.-G.; Mariscal, A. L. J.; Fierro, J. L. G.; Anderson, J. A. *J. Chem. Soc., Faraday Trans.* **1994**, *90*, 3711.
(55) Sawatzky, G. A.; Post, D. *Phys. Rev. B* **1979**, *20*, 1546.
(56) Bensalem, A.; Verduraz, F.-B.; Delamar, M.; Bugli, G. *Appl. Catal., A* **1995**, *121*, 81.
(57) Burroughs, A.; Hamnetty, A.; Orchars, A. F.; Thorntion, G. *J. Chem. Soc., Dalton Trans.* **1976**, 1686.
(58) Albero, J.-S.; Reinoso, F.-R.; Escribano, A.-S. *J. Catal.* **2002**, *210*, 127.
(59) Daturi, M.; Binet, C.; Lavalley, J.-C.; Galtayries, A.; Sporken, R. *Phys. Chem. Chem. Phys.***1999**, *1*, 1717.
(60) Fierro, J. L. G.; Soria, J.; Sanz, J.; Rojo, J. M. *J. Solid State Chem.* **1987**, *66*, 154.
(61) Damyanova, S.; Bueno, J. M. C. *Appl. Catal., A* **2003**, *253*, 135.
(62) Bukhtiyarov, V. I. *Catal. Today* **2000**, *56*, 403.
(63) Adams, C. R.; Jennings, T. J. *J. Catal.* **1970**, *17*, 157.
(64) Echigoya, E.; Sano, H.; Tanaka, M. Proceedings of the 8th International Congreso in Catálisis; Verlag Chemie: Weinheim, 1984; Vol. 5, p 62.
(65) Park, M. S.; Vislovskiy, V. P.; Chang, J. S.; Shul, Y. G.; Yoo, J. S.; Park, S.-E. *Catal. Today* **2003**, *87*, 205.
(66) Chen, M.; Zheng, H.; Shi, C.; Zhou, R.; Zheng, X. *J. Mol. Catal. A: Chem.* **2005**, *237*, 132.
(67) Reddy, B. M.; Lakshmanan, P.; Bharali, P.; Saikia, P. *J. Mol. Catal. A: Chem.* **2006**, *258*, 355.